5-2013

# Exploration of Mouth Shading and Lighting in CG Production

Chaoren Li
*Clemson University*, chaorel@g.clemson.edu

# Exploration of Mouth Shading and Lighting in CG Production

---

A Thesis
Presented to
the Graduate School of
Clemson University

---

In Partial Fulfillment
of the Requirements for the Degree
Master of Fine Arts
Digital Production Arts

---

by
Chaoren Li
May 2013

---

Accepted by:
Timothy A. Davis, Committee Chair
Tony Penna
Anderson Wrangle

# Abstract

The lighting and shading of human teeth in current computer animation features and live-action movies with effects are often intentionally avoided or processed by simple methods since they interact with light in complex ways through their intricate layered structure. The semi-translucent appearance of natural human teeth which result from subsurface scattering is difficult to replicate in synthetic scenes, though two techniques are often implemented. The first technique is to create an anatomically correct layered model, and render the teeth with both theoretically and empirically derived optical parameters of human teeth using physical subsurface materials. The second technique largely takes advantage of visual cheating, achieved by irradiance blending of finely painted textures. The result visually confirms that for most situations, non-physically based shading can yield believable rendered teeth by finely controlling contribution layers. In particular situations, such as an extremely close shot of a mouth, however, a physically correct shading model is necessary to produce highly translucent and realistic teeth.

# Dedication

I would like to dedicate this thesis to my sister, my parents, and girlfriend Stefanie, for the support and courage they gave me throughout my studies in DPA. This thesis would not be presented without you all.

# Acknowledgments

Thanks to Dr. Timothy A. Davis, my thesis advisor, for responding to my first questions about DPA, for consistent guidance, inculcation and courage during my graduate study in the DPA program, and for the wise and sincere advice in my final project, this thesis. I especially thank you for teaching me English.

I would also like to thank Dr. Jerry Tessendorf, our department chair, for bringing professional concepts of education to DPA. His concise and efficient style really influenced my study, and his efforts on guiding DPA students in their future endeavors should be appreciated by everyone in the program.

Thanks to Dr. Donald H. House and his wife - my coding and painting progressed greatly by your teaching.

Finally, thanks to all DPA faculty and students. I deeply enjoyed these years with you, as my knowledge and experience deepened, my view broadened and my circle of friends enlarged.

# Contents

# List of Figures

# Chapter 1

# Introduction

## 1.1 Mouth Processing in CG Production

Benefiting from the advancement of related techniques, production pipelines of today's movie companies are becoming mature, as specialized lighting and rendering methods have been developed to process characters. Eyes, artistically termed as the gateway of a character's soul, have been implemented independently from the face, relying on support from both technique and art. While lighting for eyes and fur has been somewhat standardized in industry production, the same specialization has not been applied to teeth processing. In the movie *Madagascar: Escape 2 Africa (2008)*, the quality of teeth is not as convincing as the characters' skin and eyes, as seen in Figure 1.1.

Figure 1.1: A shot of purely diffuse teeth from *Madagascar: Escape 2 Africa (2008)*

The properties of the mouth in Figure 1.1 are mainly diffuse, while other optics properties, such as reflection and translucence, are not as prevalent. Such an appearance makes the mouth appear dry and flat to the audience. The lack of necessary optical properties also causes an obvious mismatch between the brightness of the teeth and the illumination of the environment, i.e., the lion on the left appears to include an additional light source in his mouth that lights the space.

Figure 1.2: A shot of purely diffuse teeth from *Shrek the Third (2007)*

A second example, shown in Figure 1.2, shows the material of the teeth of Shrek as similar to ceramics. The teeth appear dry, although reflection of environmental lights is evident. Additionally, some slight yellowish speckles are presumably intended to be calculus or the inner texture of the teeth, but the optic qualities do not provide a sense of either. Finally, the audience cannot see the other parts of the inner mouth; instead the mouth appears to be a black hole absorbing all incoming light.

## 1.2 Subsurface Scattering

While the term, subsurface scattering, originated from medical and light science, it is defined more narrowly as a mechanism of light transport in which light penetrates the surface of a translucent object, is scattered by interacting with the material inside of the object, and exits the surface at a different point.

All non-metallic materials are translucent to some degree [16]. In the physical world, most materials are slightly translucent, even for materials with a solid appearance, such as pebbles. Skin is a good case here; for neutral skin, only about 6% of reflectance is direct, while the remaining 94% is from subsurface scattering [16]. Light that enters the surface is absorbed, scattered and re-emitted potentially from a different point; the further through the material it travels, the greater the proportion absorbed [4]. Figure 1.3 shows actual subsurface scattering of grapes and simulation of subsurface scattering on marble.

(a) Grapes [8] (b) Marble by BSSRDF approximation [16]

Figure 1.3: Examples of subsurface scattering

## 1.3 Brief Mouth Anatomy

The roots of teeth are embedded in the maxilla (upper jaw) or the mandible (lower jaw) and are covered by gums. The root is covered by a structure called cementum. The area where enamel and cementum meet is called the cement enamel junction (CEJ). Similarly the interface between the enamel and dentin in the crown is called the dentin enamel junction (DEJ). The soft central core made up of connective tissue is called pulp, as shown in Figure 1.4.

Enamel (Figure 1.5) envelopes the crown section and is primarily composed of an organized array of inorganic hydroxyapatite crystals, $Ca_{10}(PO_4)(OH)_2$, arranged in keyhole-shaped prisms surrounded by a protein, lipid and water matrix forming the inter prismatic. Healthy enamel is translucent, primarily from the crystalline prismatic structure and its composition.

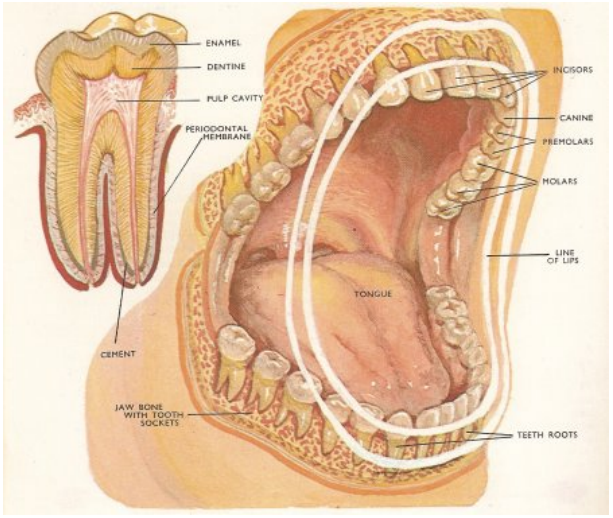


Figure 1.4: Mouth of an adult and the structure of a molar, courtesy David Darling

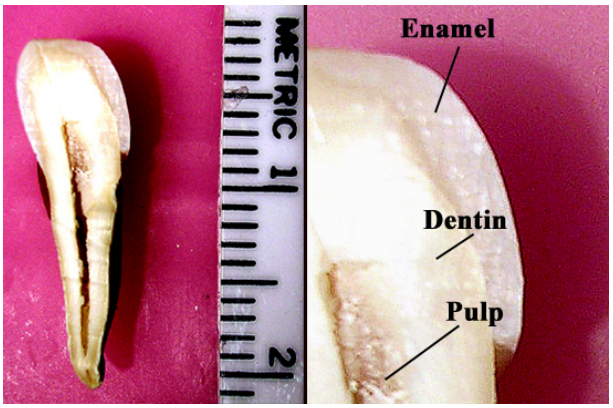


Figure 1.5: Intersection of an adult molar [27]

Dentin, which is less mineralized and less brittle than enamel, is necessary for the support of enamel [19]. Seventy percent of dentin weight is hydroxylapatite, twenty percent is organic material and the rest is water. Its yellowish appearance greatly affects the color of teeth due to the high translucency of enamel [26]. In dentin, tubules are the primary scattering component; the diameter and density of dentin tubules decrease towards the dentin enamel junction. The orientation of the tubules with respect to an incident beam of light gives rise to the anisotropic response of teeth [1].

## 1.4 Optical Properties of Subsurface Scattering

The important optical properties which govern light interaction of translucent materials are as follows:

- The index of refraction (ior), or $n$, determines how light changes direction as it enters or leaves the material. The ior of materials varies along the spectrum of wavelength. In opaque media, the refractive index is described as a complex number; the real part is the refraction, while the imaginary part stands for the absorption [28].
- The absorption coefficient ($\mu_a$) is a measure of the attenuation of light as it travels through a turbid media [10]. It is wavelength-dependent and usually expressed in units of inverse length; hence, the product of the absorption coefficient and path length of a photon's travel through the media is dimensionless.
- The scattering Coefficient ($\mu_s$) describes a medium containing many scattering particles at a concentration of volume [22]. It depends on both composition of the material and wavelength of incident light. The scattering coefficient is essentially the cross-sectional area per unit volume of medium.
- The anisotropy factor ($g$) is a measure of the degree of scattering [10]. It is calculated from the average dot product between the direction of incident light and of the scattered light. Most turbid materials do not scatter light uniformly. The mean free path length is the average distance a photon will travel in the material without scattering or absorption and is equal to the reciprocal of the sum of the scattering and absorption coefficients (units of length should match before inverse) [10].

### 1.4.1 Outline Of Thesis

Background of shading methods and related anatomic content are introduced in Chapter 2. In Chapter 3, the implementation of methods discussed in Chapter 2 are covered in detail. Chapter 4 shows the resulting images, and Chapter 5 concludes the thesis and proposes potential future work found during the research.

# Chapter 2

# Background and Methods

This chapter provides a general guide for shading teeth, and covers several important aspects from both technical and artistic perspectives. It also analyzes the current methods of digital rendering.

## 2.1 Physical Shading Guide for Teeth

In computer graphics, separating contributions of diffuse, scattered and reflected colors of teeth is challenging since they exhibit various phenomena which are difficult to represent accurately. Apart from surface and subsurface reflection and refraction, teeth also exhibit fluorescence[12], birefringence effects [17] and angular dependency.

Tooth color is determined by the paths of light inside the tooth and absorption along these paths, and since the paths are determined by scattering, a relation between color and scattering coefficients exists [9]. The study of J.J. ten Bosch quantitatively confirms that tooth color is mainly determined by dentin, where enamel plays only a minor role through scattering light at wavelengths in the blue range under the spectrum of visible wavelength range.

An absorption spectrum measured from a thinly sliced non-carious tooth is shown in Figure 2.1. The decrease in light is due to absorption and light scattering in the tooth. The peak near 750nm is probably due to the contribution of proteins [24].

The light source being used is one of the most important, but frequently one of the most neglected, aspects of shade selection [6, 15]. Artificial light is almost universally used in dental

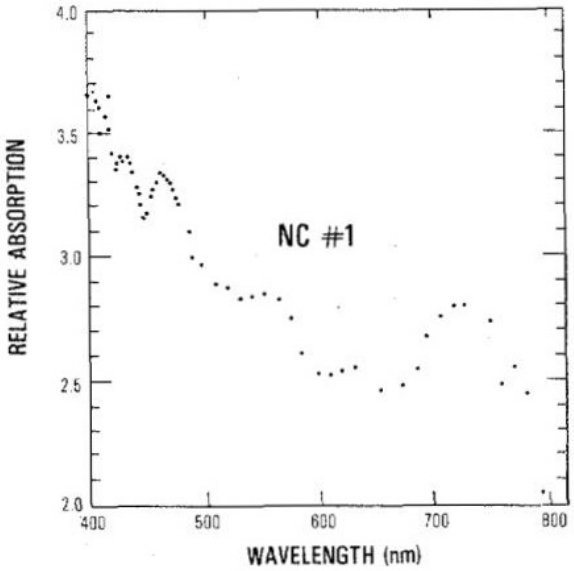


Figure 2.1: Relative absorption spectrum for a non-carious tooth [24]

surgeries. It can be incandescent (which emits a higher concentration of yellow light) or fluorescent (which emits higher concentrations of blue light). Neither of these is pure white light [5]. Duplicating a natural light source is almost unachievable based on current technology. The standard way to achieve high quality lighting is to use a light rig similar to studio lighting, with 6500K light color. The two layers of the tooth surface that affect the interaction of light are enamel and dentin.

### 2.1.1 Enamel

Translucency, the relative amount of light transmitted through a material, is the most important attribute in shading teeth realistically. The transmission coefficient associated with a tooth surface is a measure of translucency, defined as the relative amount of light passing through the unit thickness of the material. A detailed analysis of translucency of enamel (shown in Figure 2.2) was performed by [20]. This study shows that the total transmission is directly proportional to wavelength, i.e., human tooth enamel is more translucent at higher wavelength. It also matches well with scattering analysis which shows higher scattering at lower wavelengths.

The density of enamel decreases towards the dentin, and is characterized by slight absorption over the visible wavelength. Its scattering coefficient decreases with increasing wavelengths. High scattering at lower wavelengths is attributed to dimensions of crystals resulting in Rayleigh

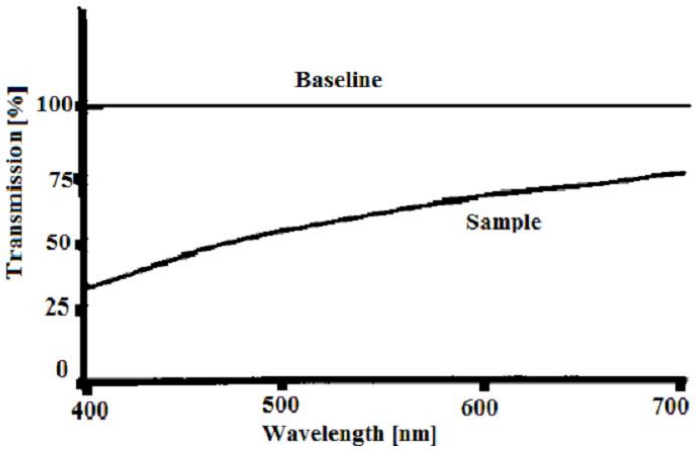


Figure 2.2: A wavelength-dependent transmission [20]

scattering; hence a blue tint exists in teeth where dentin is absent. Its scatter coefficient $s$ decreases from 9 to 1.5 $mm^{-1}$ as wavelengths increased from 400 to 700nm. The absorption coefficient $k$ almost equals 0.1 $mm^{-1}$ over this wavelength region [11].

### 2.1.2 Dentin

The light entering teeth is either absorbed or scattered. Scattering coefficients are independent of mineral content in dentin, but dependent on transmission in enamel. A model containing scattering by crystals and by prisms was presented. It shows that the prisms are the most important scatters but that the crystals are responsible for the back scattering [18]. Some other experiments carried out to determine optical properties of dentin are magnification effect of dentin tubules [3], anisotropy dependence [2], dentin polarization effects [25] and optical coherence tomography imaging technique [31]. The composition and structure of dentin is discussed in detail in [31], [25] and [14]. Figure 2.3 shows the scattering coefficient and anisotropy coefficient over the visible wavelength.

## 2.2 Shading Guide for Gums

Anatomically, gums are composed of three layers: marginal, attached and inter-dental areas, which represent the terminal edges of gums surrounding the teeth, the continuous tissue in-between the marginal layer and the alveolar bone beneath, and the interproximal space beneath the area of tooth contact, respectively. Healthy Gums are usually coral pink, but may contain physiologic

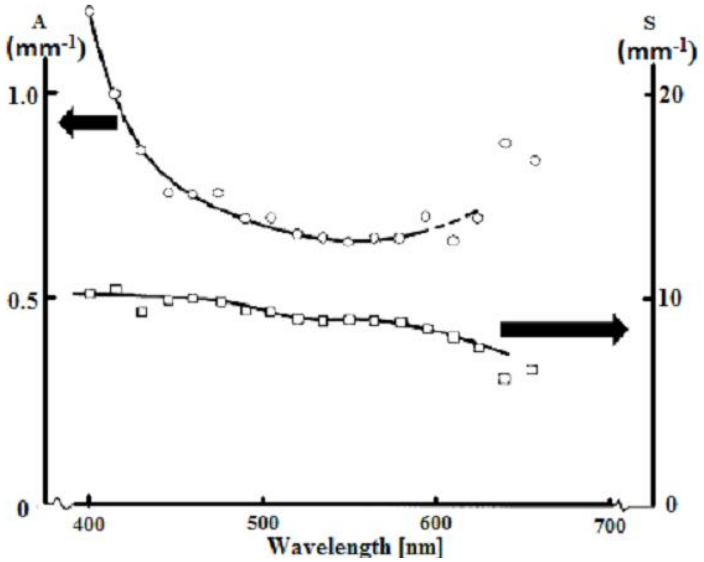


Figure 2.3: Scatter ($s$) and anisotropy coefficient ($a$) over visible wavelength (400nm - 700nm) [7]

pigmentation. Besides the color, other visual characteristics of gums are texture and contour, which is the smooth fan-shaped appearance around each tooth, fully filling each inter-dental space. Gums have a firm texture that is resistant to movement, and the surface texture often exhibits surface stippling where the attached gums are bound to the alveolar bone, as shown in Figure 2.4.

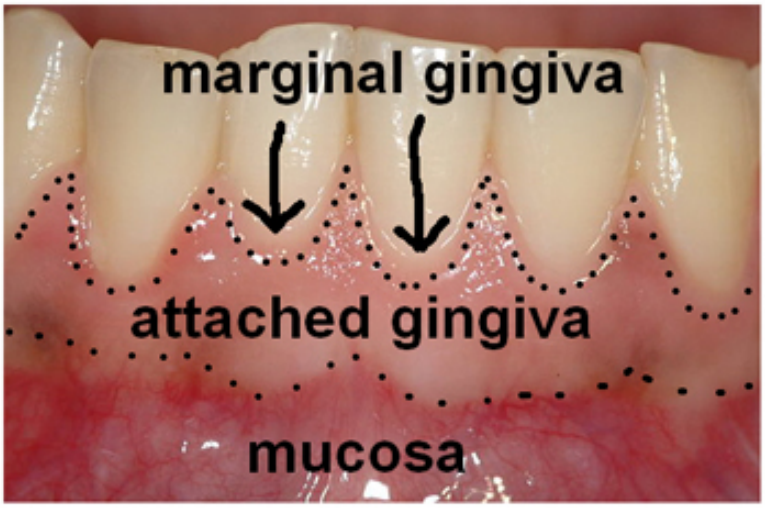


Figure 2.4: Healthy gums show complex tissue texture [13]

## 2.3 Subsurface Scattering in Computer Graphics

Currently two methods are commonly used in rendering subsurface scattering. The non-physical type, which results in faster rendering speed but less physical accuracy, includes rendering techniques such as depth map-based method. The physical type includes photon mapping and BSSRDF (bidirectional surface scattering reflectance distribution function) approximation.

### 2.3.1 Non-physical Subsurface Scattering

Non-physical models do not simulate true volumetric scattering. Limitations on precise transmission control and crystalline refraction become evident when rendering high scattering inorganic materials. Such techniques have therefore been mainly applied on shallow scattering materials such as skin and flesh.

### 2.3.2 Jensen's Physical Scattering Models

Danish computer graphics researcher Henrik Wann Jensen has made several important contributions in the area of photo-realistic light transport including the photon mapping technique for global illumination, subsurface scattering in translucent materials and simulating physically correct light properties on a 3D object. Photon mapping as a physically correct simulation is useful for simulating subsurface scattering, but it becomes expensive for highly scattering materials such as jade and skin. In its standard implementation, photon mapping is a two-pass global illumination algorithm.

The first pass is the construction of the photon map. Typically, caustics photon maps and global illumination photon maps are created separately. After intersecting the surface, a probability for reflecting, absorbing, or transmitting/refracting is decided by the material. A Monte Carlo method called Russian roulette is then used to choose one of these actions. Similar to physical photon transport, if the photon is absorbed, no bounce direction is computed, and tracing for that photon ends. If the photon reflects, the surface's BRDF (bidirectional reflectance distribution function) is used to determine the ratio of reflected radiance. Finally, if the photon is transmitted, a function for its direction is given depending upon the nature of the transmission.

The second pass evaluates the radiance of every pixel of the output image. Each pixel is ray traced to compute the closest intersection point. The rendering equation is then used to calculate

the surface radiance, leaving the point of intersection in the direction of the ray that struck it. Four separate factors from the equation are used to calculate contributions to the pixel: direct illumination, specular reflection, caustics and soft indirect illumination.

Photon mapping is a "biased" rendering algorithm, which means that averaging many renders using this method does not converge to a correct solution to the rendering equation. Since it is a consistent method, however, a correct solution can be achieved by increasing the number of photons. Additionally, Jensen introduced a rendering model using BSSRDF, an alternative to Monte Carlo methods, that led to a new techniques based on diffusion approximation [16].

## 2.4 The misss_physical Shader in mental ray

The misss_physical node (physical subsurface scattering shader) simulates the volumetric scattering of light beneath the object's surface. It uses a photon map (*kd-tree*) assigned to the object to store the photon information. The misss_physical shader performs three types of simulation: single-scattering, diffusion, and multiple-scattering, as shown in Figure 2.5. Single-scattering approximation is based on light intensities, independent of photon mapping. Diffusion theory is applied to evaluate the contribution of photons in the deep layer. Multiple-scattering estimation is the most accurate, using a strictly deterministic simulation of photon tracing to record sites in an internal photon map. Each simulation functions independently. Depending on the optical properties of the material, the contributions of each component may dominate or be negligible.

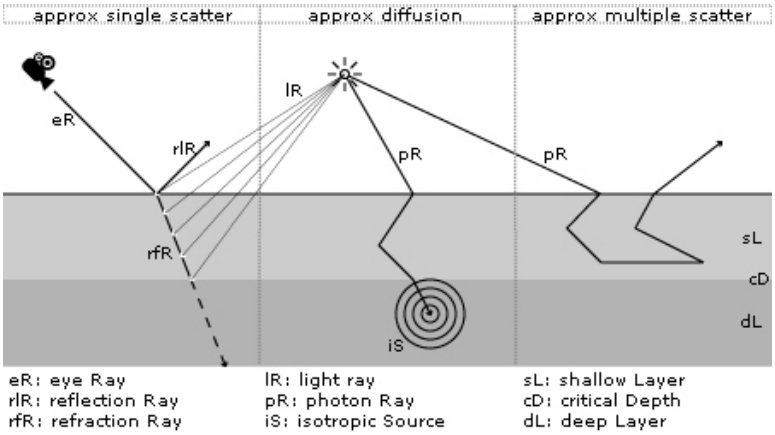


Figure 2.5: Three types of approximation in misss_pysical shader [10]

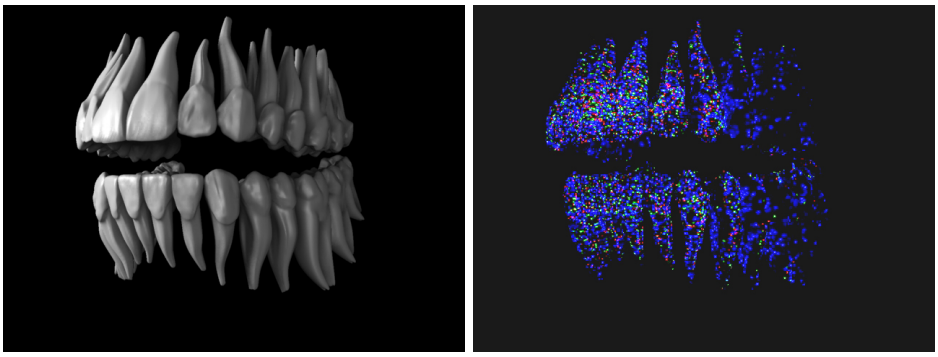

(a) Bare teeth model (b) Distribution of photons

Figure 2.6: Rendering with optic parameters set as enamel

Since the misss_physical shader is based on photon mapping, the optical properties of teeth discussed previously are all controllable, and may vary since they are empirically derived by different methods and institutions. As a result, matching the scale of the parameters is critical to achieve correct volumes for computing; in our case, the coefficients are expressed in units of inverse millimeters. The shader computes the final color by blending color data stored in the photon maps; hence, parameters such as maximum number of samples and radius of photon affect the computation largely, both in terms of rendering quality and time.

Figure 2.6a presents a view of human teeth. Figure 2.6b shows photons inside of the model after photon mapping. At each 3D location inside the model, the photon shader stores data about the incoming light. Each photon can bounce inside, scattering and storing light information multiple times within the model.

## 2.5 The misss_fast_skin_phen in mental ray

The misss_fast_skin_phen is a predefined shading network based on the misss_fast_shader. The term *phenomenon* in mental ray refers to a shading network which consists of mental ray shaders. Three important features of this type of non-physical shader include: a special data structure called lightmap to store diffuse irradiance, and later to simulate scattering; two types of scattering, front and back, determined by camera space; and independence from other global illumination techniques such as photons, caustics and ray tracing. Besides diffuse and specular components, the scatter component simulates light scattering at the subsurface level when it ceases at the surface. For each of the scattering components, a radius parameter controls how the distance to the light affects scat-

tering along the surface. An additional parameter, depth, controls the depth the light can travel in materials according to camera perspective. The front scattering is divided into an epidermal layer and a subdermal layer, which present the whitish/yellowish layer just under the surface and the deeper reddish/orangeish flesh layer, respectively, as shown in Figure 2.7. All components are then added through a soft add method, as shown in Figure 2.8.

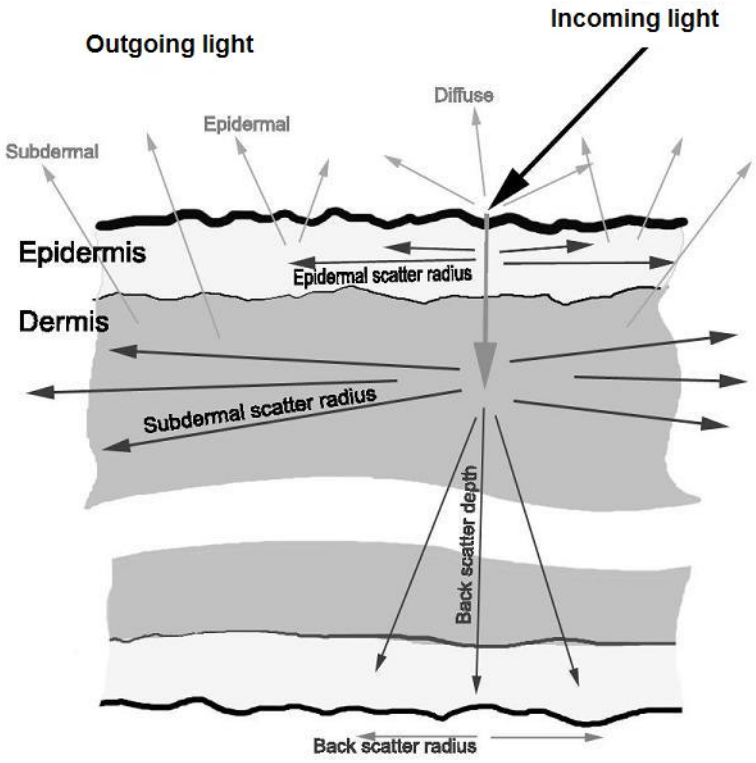


Figure 2.7: Visualized parameters of misss_fast_skin_phen [10]

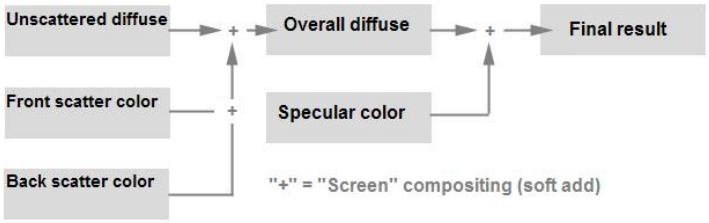


Figure 2.8: The color computation of misss_fast_skinphen [10]

## 2.6 Color Management, Gamma Correction and Linear Workflow

As discussed previously, the high scattering quality of both teeth and flesh determines that subtle changes of light and color do affect the final appearance. In order to ensure that that color remain unbiased during rendering, it is critical to keep color data linear during the processing, which is commonly referred as Color management. The primary goal of color management is to obtain a good match across color devices; e.g., the colors of one frame of a video should appear the same on a computer LCD monitor as on a plasma TV screen. Color management occurs across several steps during media processing. First, characterization and calibration ensure close, or ideally the same, color performance on various display devices. Second, image or video require embedded color profiles to in force the post-editing software which working color space should be chosen, in order to interpret the color data correctly. Third, color transformation, occurs when need for translating a color from one space to another [29].

Gamma correction, or simply gamma, is the name of a nonlinear operation used to code and decode luminance or tristimulus values in visual media formats. It commonly occurs during the second and third steps of color management. sRGB, created cooperatively by HP and Microsoft in 1996, is a standard RGB color space used in current industry for use on monitors, printers. Although sRGB gamma cannot be expressed as a single numerical value, the overall gamma is approximately 2.2, consisting of a linear (gamma 1.0) section near black, and a non-linear section elsewhere involving a 2.4 exponent and a gamma (slope of log output versus log input) changing from 1.0 through around 2.3 [30].

Linear workflow is now a standard production workflow to maintain linear transfer of luminance and color data throughout the pipeline. Basically, data are generated linearly, and processed linearly until the final output. If data are not generated linearly, a gamma correction should be applied before editing. Additionally, a gamma correction for display, usually to sRGB, operates independently.

# Chapter 3

# Related Work

This chapter provides information about the materials needed for rendering teeth. It describes the implementation of the two methods, which have been introduced in Chapter 2, and discusses advantages and disadvantages of each during the process.

## 3.1 The Mouth Model

A base model of human teeth was used for exploration purposes in the implementation of the teeth shader. The model was generated by a CT scan of a healthy mouth of an adult male. Over 100,000 quad-faces were included, which were highly detailed and sufficient to represent the interior structure of the mouth for shading purposes. The width of teeth from left to right was 83.2cm; the depth from front to back was 8.17cm. The UV map covering every part of the model was created with UV Layout in a strict proportion ratio and in a well-organized way. The teeth, gums and tongue were separated in geometry groups, with each sharing a UV map.

## 3.2 Shading with Non-physical Material

All materials applied in this method are non-physically based. Due to the subsurface scattering characteristics of organic materials, the shading network was based on misss_fast_* shaders.

### 3.2.1 Setting up Lights

Two direct light sources were placed in the scene as a key light and a fill light. For better reflections, an environment sphere was added, with light distribution similar to physical lights. Final gathering was activated, but was only apparent when an object was placed in the mouth.

### 3.2.2 Texturing and Shading Gums

According to Figure 2.4, which labels the elements of the gums, the epidermal layer is an intertwined layer of oral epithelium and alveolar mucosa. The thickness of this layer is approximately 1/15 of the attached gums, or 0.1-0.2mm. As a result the texture of this layer is highly translucent and tinted by cells and other organic materials. The color of the epidermal layer does not show distinctly perpendicular to the perspective because of intense subsurface scattering, but appears at half brightness, near the marginal areas, as a topaz color.

The subdermal layer is mainly subepithelial connective tissue. This layer is the location where diffuse scattering contributes to the visual characteristics discussed in Chapter 2. Extending to the root area, the color of the gums exhibit more red blending since the modena and blood capillaries reside within the hypoglossal and palate canal. Thick blood veins may be exposed, contributing greatly to the visual qualities of this layer. For realistic open-mouth rendering, several detailed internal oral surfaces are needed. For example, ridges on maxilla caused by the hard and soft palates with color desaturation and dense areas of nerve and blood veins around the tonsil and posterior wall of the oropharynx must be included.

Back scattering was also handled carefully. The thickness of the gums varies from 0.8mm to 4mm. Consider the incoming light angles and underlying bones, the most likely areas where back scattering could occur are the regions in between the teeth and lips. Other contribution maps include diffuse, bump and specular, as shown Figure 3.1.

In the misss node, the epidermal depth was set to 0.15mm, with the scatter radii of the subdermal layer and back scattering radii were set to 3mm based on physical measurements. Additionally, the depth of back scattering was set to 3mm corresponding to its radius. If the light hits a tooth, therefore, the scattering will affect the gums of the neighboring teeth.

The color component from scattering was plugged into a mia_material_x node, which conserves light energy to achieve a more accurate and controllable reflection and surface bump. In

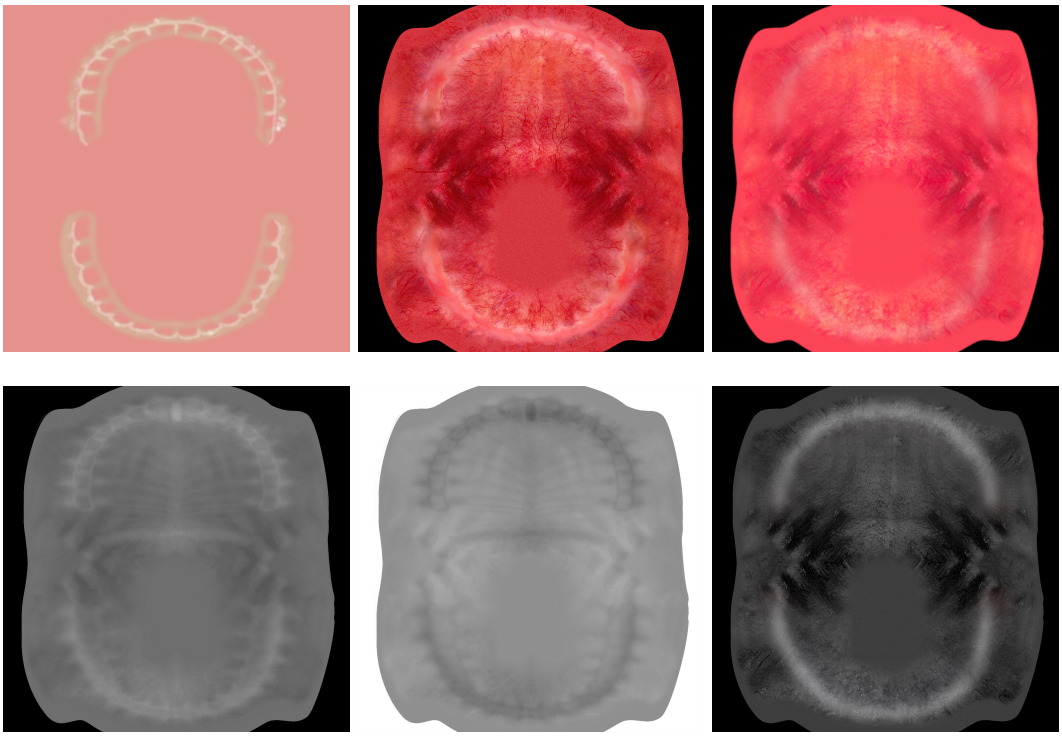

Figure 3.1: Epidermal, subdermal, back, diffuse, bump and specular maps used for the gums shading network

order to activate the misss node, a light map node was also plugged into the shading group of the mia node as shown in Figure 3.2. Each contribution map was connected to a corresponding entry, and because the bump affects the irradiance map, plugged into a misss node also. With a similar procedural, the shading network for the tongue was created as in Figure 3.3, without back scattering.

### 3.2.3 Texturing and Shading Teeth

One of the advantages of the misss shader is the ability to control color on a channel basis; therefore, analysis of color from perceptual and visual aspects is critical to determining the final look of rendering.

#### 3.2.3.1 Color Transition of Teeth

Given the images in Figure 3.4, colors are extracted and enhanced separately in red and yellow components. Due to the highly translucent quality of enamel, color bleeding from the gums tint the areas close to the gums and areas which do not contain dentin underneath with a reddish

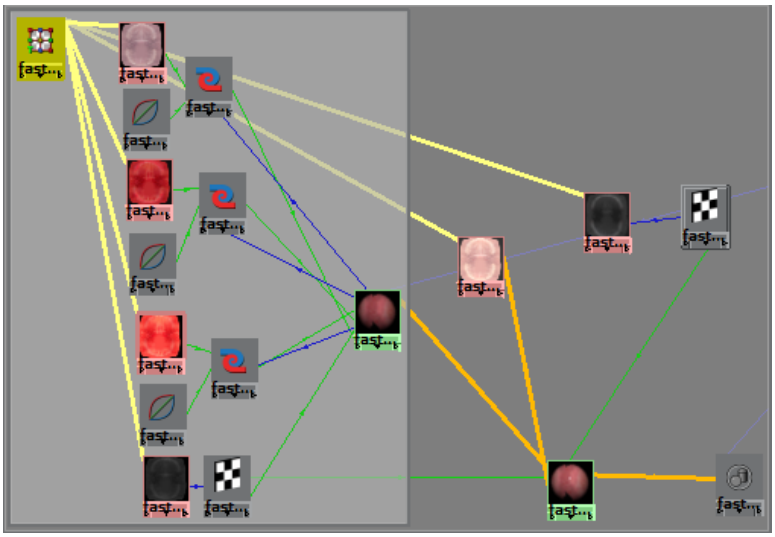

Figure 3.2: Shading network of gums

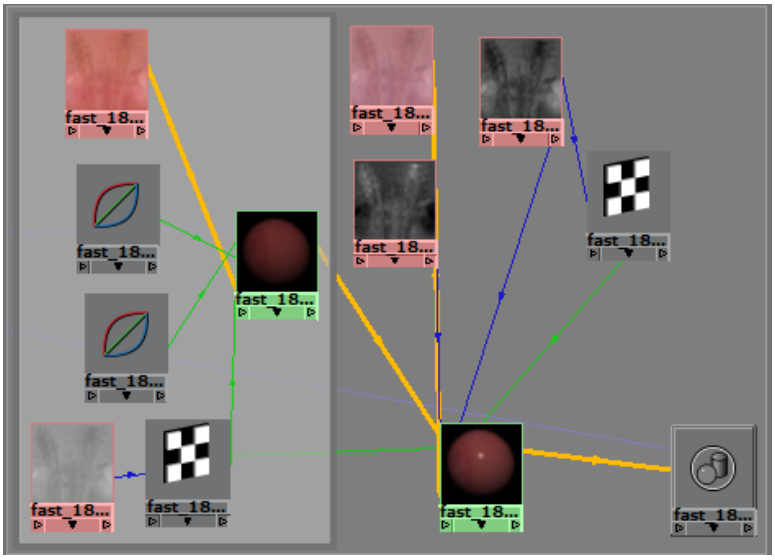

Figure 3.3: Shading network of tongue

color, as shown in Figure 3.4b. The distribution of dentin can be seen partially in Figure 3.4c, where areas that appear more yellowish indicate thicker dentin underneath. Conversely, areas appear darker and more transparent where little or no dentin lies underneath, thereby reducing light scatter. As described in Chapter 2, enamel greatly scatters blue light, a color complement to yellow. Light areas that appear darker and more transparent also indicate that enamel more strongly influences scattering.

Other environmental factors could also influence the color of teeth, including the lips, caries

(a) Natural color under white light (b) Regions contain red (c) Regions contain yellow

Figure 3.4: Isolating colors of the teeth

and calculus, which were not considered in this model. The light source color was another critical factor for this particular method, since no global illumination techniques were used here. Any light color other than white may therefore cause unexpected output results.

#### 3.2.3.2 Texturing Teeth

According to the computational method of the misss phenomenon and teeth anatomy, the epidermal texture, which represents the enamel here, exhibits the optical qualities of pure enamel: a blue tinted material with a cloudy interior developed during formation, as shown in Figure 3.5.

The subdermal layer contains all of the possible visual qualities beneath enamel, including: transmission color and diffuse color of dentin, color bleeding from the gums and tongue, and variations at areas where different surfaces, such as teeth and gum, meet. Another opacity texture was used to control the presence and weight of dentin. For human teeth, those areas mainly appear on incisors and canines, as shown in Figure 3.6 .

An imaginary texture for back scatter is shown in Figure 3.7a. The expected result is a dim light highly scattered by the pulp and other organic structures beneath the dentin. In the hollow areas of teeth, a multitude of nerves and blood result in light filtering and scattering toward the rad range. Other textures that where applied include a bump map and a dirt map as shown in Figures 3.7b and 3.7c. The bump map added variety to reflections, diffuses and scattered light, to simulate the uneven surface of teeth during formation. The dirt map provided a more natural sense

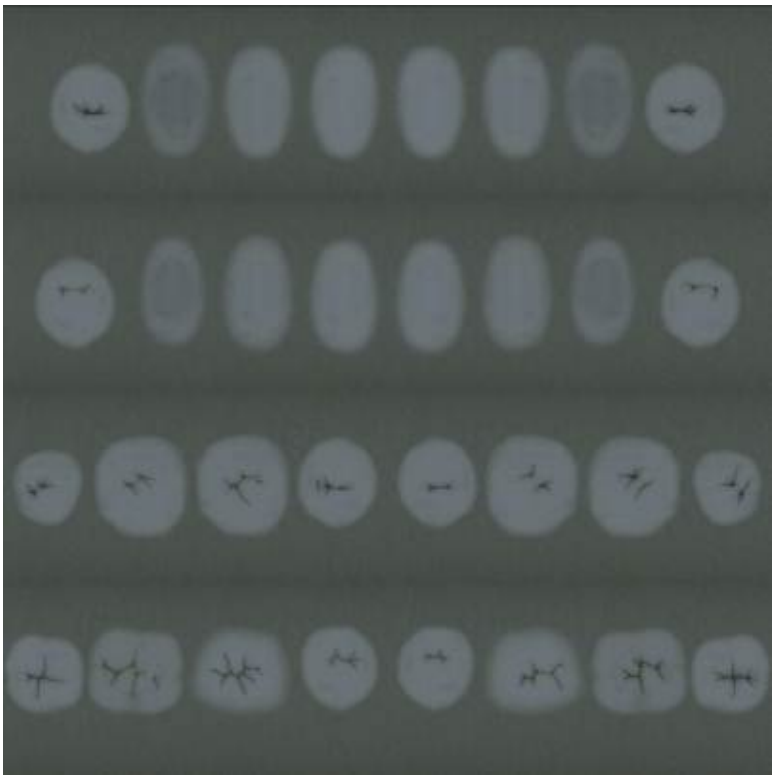

Figure 3.5: Epidermal map

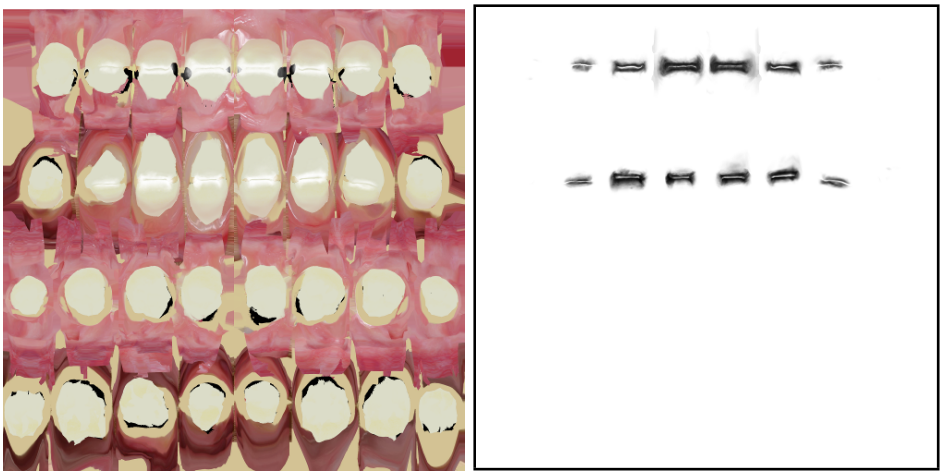

(a) Subdermal map (b) Weight map for subdermal layer

Figure 3.6: Maps for subdermal scattering

and variety to the surface level.

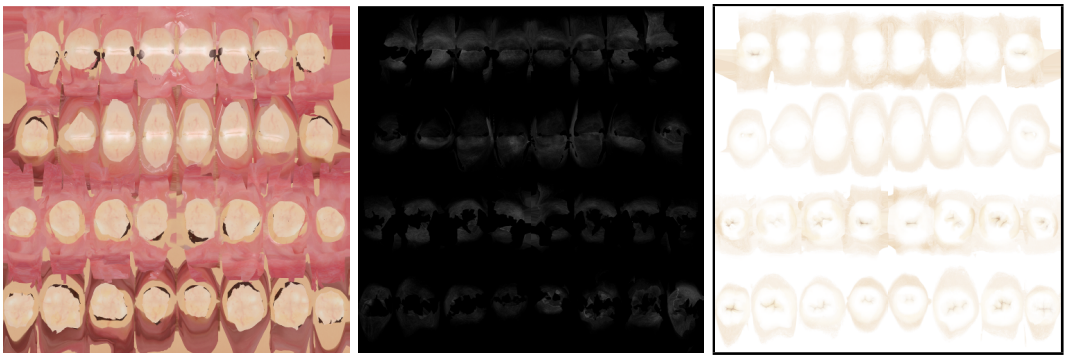

(a) Back scattering map (b) Bump map (c) Dirt map

Figure 3.7: Isolating colors of the teeth

#### 3.2.3.3 Wavelength-dependent Shading Network

Since the misss phenomenon is not energy-conservative with a limited control of reflection, only the scatter color part of its output was used. For obtaining wider color in post-processing, each component of the scatter color was plugged into a duplicated phenomenon which is scaled by a corresponding weight. A color correction node, which corrected the component according to the scattering coefficient was then added before written into the frame buffer. The corrected scattering colors were then plugged into a mia_material_x as additional colors. In order to make the scattering work for the mia node, the lightmap node was connected to the shading group of the mia node. In the final step, all scattering colors were totaled by a mib_color_mix, as shown in Figure 3.8.

#### 3.2.3.4 Artifacts of the misss_fast_skin shader

In shading tests, an unwanted effect appeared due to the two-front-layer phenomenon. A separate model is used for showing the effect more distinctly, as shown in Figure 3.9. The light scattering around shadow terminators does not appear smooth due to over-weighting of the front or mid color.

The technique for blending data stored in the lightmap is not obvious. The phenomenon blurs the terminator towards both directions, and multiplies with scatter color. Areas beyond the front radius, but still in the range of mid radius, have the full weight of the front color and the multiplied weight of the mid color; as a result, these areas appear more reddish in the final render.

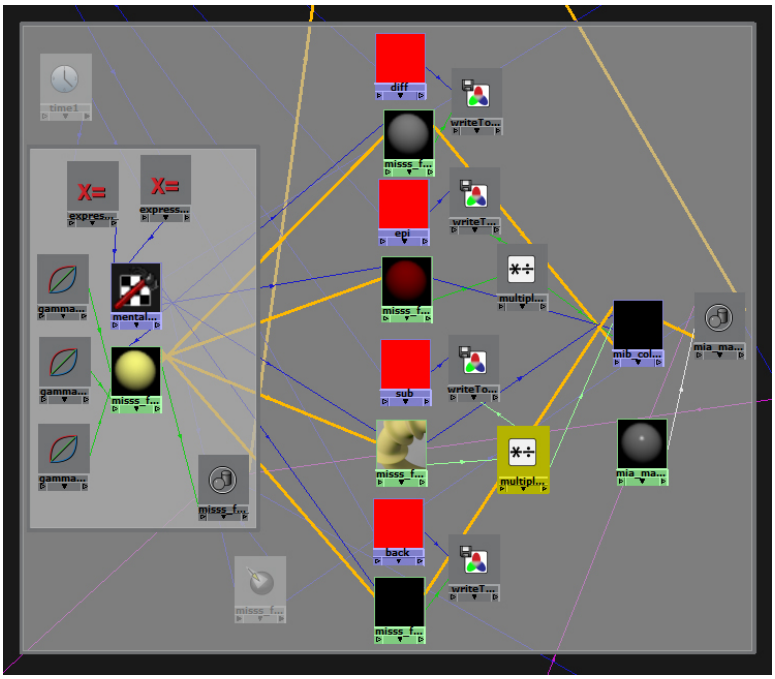


Figure 3.8: Advanced layered shading network for teeth

## 3.3 Shading with Physical Material

According to the cross section of teeth shown in Figure 1.4, a single tooth contains three actual layers: enamel, dentin and pulp, from outside to inside. The misss_physical shader is applied to both the enamel and dentin layers, as discussed in Chapter 2, since the two organic materials actually act as an inorganic material with a well-ordered micro-structure.

### 3.3.1 Limitations of the misss_physical shader

Three critical limitations were found during the preparation of the scene. These limitations of the current photon-mapping scattering model in mental ray have not been addressed in the past five years, and are not expected to change in the near future.

First, since the misss_physical shader performs scattering along the geometry, it requires objects to include both entering and exiting surfaces in order to store photons correctly. Under this scheme, open meshes could cause problems. For the same reason, achieving a physically correct structure requires a precise layered model, consisting of three separately closed models extremely close to one other. Obtaining such a model was not feasible.

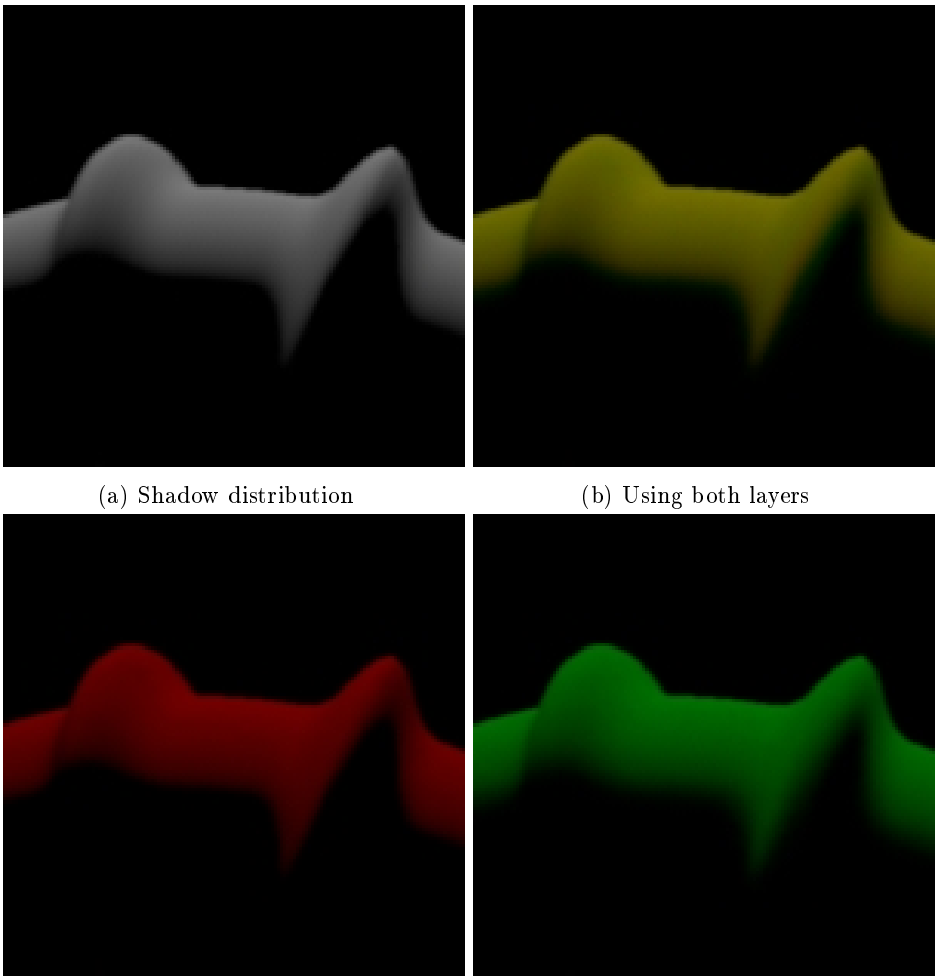

(a) Shadow distribution (b) Using both layers

(c) Epidermal layer (d) Subdermal layer

Figure 3.9: Comparision of the epidermal layer with weight = 0.5 and radius = 0.5, and the subdermal layer with weight = 0.5 and radius = 1.0

Second, the misss_physical shader does not work with the misss_fast_* shaders, which are recommended for flesh materials. Currently, the surface will render a volumetric material if the surface color is black, which causes the lightmap to be unable to find any surface directly illuminated and render it as black. The solution used a mia_material shader instead of misss_fast_* shaders for photon bounce, and composited the resulting image for the gums.

Third, the Fresnel coefficient, which controls reflectivity and refractivity depending on an ior angle (viewer/normal), is always activated in a misss_physical shader. The ior value was therefore set to 1.0 to minimize the impact of the Fresnel effect, and a second reflection layer was added to better control the reflection. This factor did not affect the render significantly since it can be masked

out.

### 3.3.2 Setting up Lights

Setting up the lights for the physical shader was more complex than in the non-physical approach. A physical sky and sun environment was added to the scene to guarantee that the color of the light sources were close to natural light. The luminance of the sky was calculated automatically based on the haze level, according to the CIE standard. To simulate an indoor light condition, a huge black sphere was created to enclose the teeth model and three portal lights were introduced to transmit the outside light into the sphere. The portal light collected light rays from the sky similar to a window, emitted photons, and maintained photon energy in a physically correct way. Three lights were each one meter from the model in a traditional three point lighting setup. Additionally, in order to blend warm and cold light, the key light, set on the left side of the camera, emitted warm light from the sun, while the other two lights transported cold lights from the sky. Final gathering, global illumination and caustics were all activated to enable environmental lighting and photon mapping.

### 3.3.3 Physical Shading of Enamel and Dentin

Shading and rendering are only implemented on enamel and dentin, so that the limitations discussed above will not appear in final frames. Based on age-related changes in tooth enamel as measured by electron microscopy[23], the thickness of the crown enamel was tweaked to an average value around 1.6mm, with a smooth decrease to the side line below the marginal gums. The thickness of dentin was approximately three times that of enamel, of which the average value of the crown side was 5mm, which enveloped the pulp entirely. For better quality, depth was increased to 10 scattering events, and max_samples was increased to 32. As rendering progressed, the number of the nearest neighbor photons and the search radius were reduced to a minimum in the process of reaching the desired quality.

Two scripts shown in Figure 3.10 were run to input parameters to each shader. The optical parameters use experimentally derived values from the study in Chapter 2, but did not need to be normalized. Since over 95% of the color of enamel results from scattering, the material color was set to dim grey, and average values for dentin color, converted from CIE L*,a*,b* values of 69.9, 1.22,

and 17.9[9], were 185.39, 168.98, 139.47 in red, green and blue, respectively. No texture was used because it may have produced an unpredictable result.

This Chapter described two methods of rendering based on the discussion in Chapter 2, and covered important steps in detail. For the unexpected limitations, alternative approaches were introduced. The resulting images will be shown and discussed in Chapter 4.

```
shader "teeth_enamel_physical_sss"
        "misss_physical" (
                "material" 0 0 0 1.,
                "transmission" 0.25 0.25 0.25 1.,
                "ior" 1.61,
                "absorption_coeff" 0.01000.01000.0142,
                "scattering_coeff" 2.61 3.72 13.0,
                "scale_conversion" 1.0,
                "scattering_anisotropy" 0.7,
                "depth" 10.0,
                "max_samples" 10.0,
                "max_photons" 2000,
                "max_radius" 12.0,
                "approx_diffusion" on,
                "approx_single_scatter" on,
                "approx_multiple_scatter" on,
                "lights" [
                "keyLight"
                "fillLight"
                ]
        )
```

```
shader "teeth_dentin_physical_sss"
        "misss_physical" (
                "material" 0 0 0 1.,
                "transmission" 0.5 0.5 0.5 1.,
                "ior" 1.61,
                "absorption_coeff" 0.01000.01000.0142,
                "scattering_coeff" 2.61 3.72 13.0,
                "scale_conversion" 1.0,
                "scattering_anisotropy" 0.7,
                "depth" 10.0,
                "max_samples" 10.0,
                "max_photons" 2000,
                "max_radius" 12.0,
                "approx_diffusion" on,
                "approx_single_scatter" on,
                "approx_multiple_scatter" on,
                "lights" [
                "keyLight"
                "fillLight"
                ]
        )
```

Figure 3.10: Material scripts for enamel (top) and dentin (bottom)

# Chapter 4

# Results

This chapter shows the resulting images from the two different approaches discussed previously, and analyzes the visual difference between them. For production purposes, other possible situations were considered such as dental calculus. The rendered mouth was tested on actual models as well.

## 4.1 Physically Rendering Tooth Models

As mentioned previously, only the enamel is physically rendered due to limitations of the shader class. The diffuse-only image, Figure 4.1a, shows the distribution scale of light and shadow. Adequate quality is obtained from the misss_physical shader for natural edge scattering of enamel, as seen in the uneven and translucent pattern caused by the shape of the geometry, Figure 4.1b. The final image Figure 4.2, composited from a gum layer rendered non-physically, an enamel scatter layer and a tooth layer, imitates the qualities of real teeth. Several features, such as reflection, translucency and scattering, appear as discussed previously.

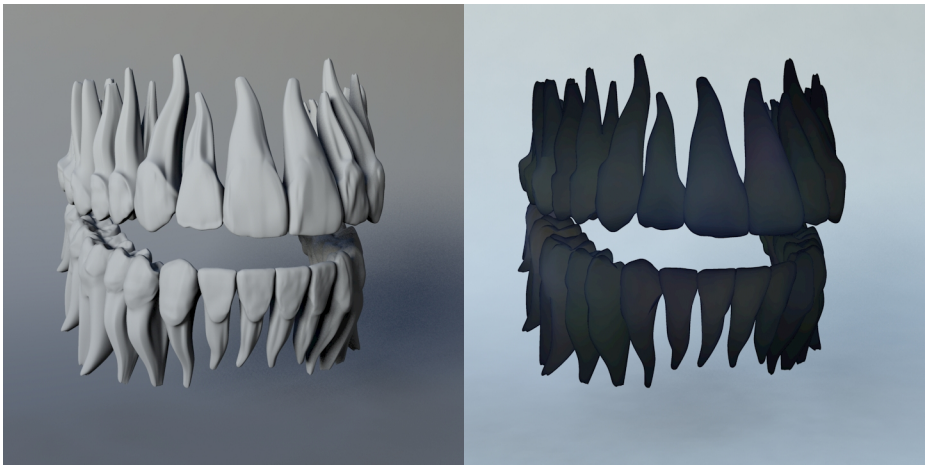

(a) Diffuse illuminated (b) Enamel Scattering

Figure 4.1: Teeth rendered with enamel scattering

Figure 4.2: Teeth rendered in a physical process, composited with tongue and gums rendered in a non-physical process

## 4.2 Non-Physically Rendering Tooth and Mouth Models

Compared to physical processing, non-physical rendering offers more control and shorter render time, since it does not need to incorporate global illumination and it is not a volumetric rendering. The gums in Figure 4.3 show a satisfactory degree of scattering. The teeth affect the color of the gums at each tooth base, and veins under the mocusa and epidermal appear to display realistic translucence, reflection and surface bump to add a sense of organic material.

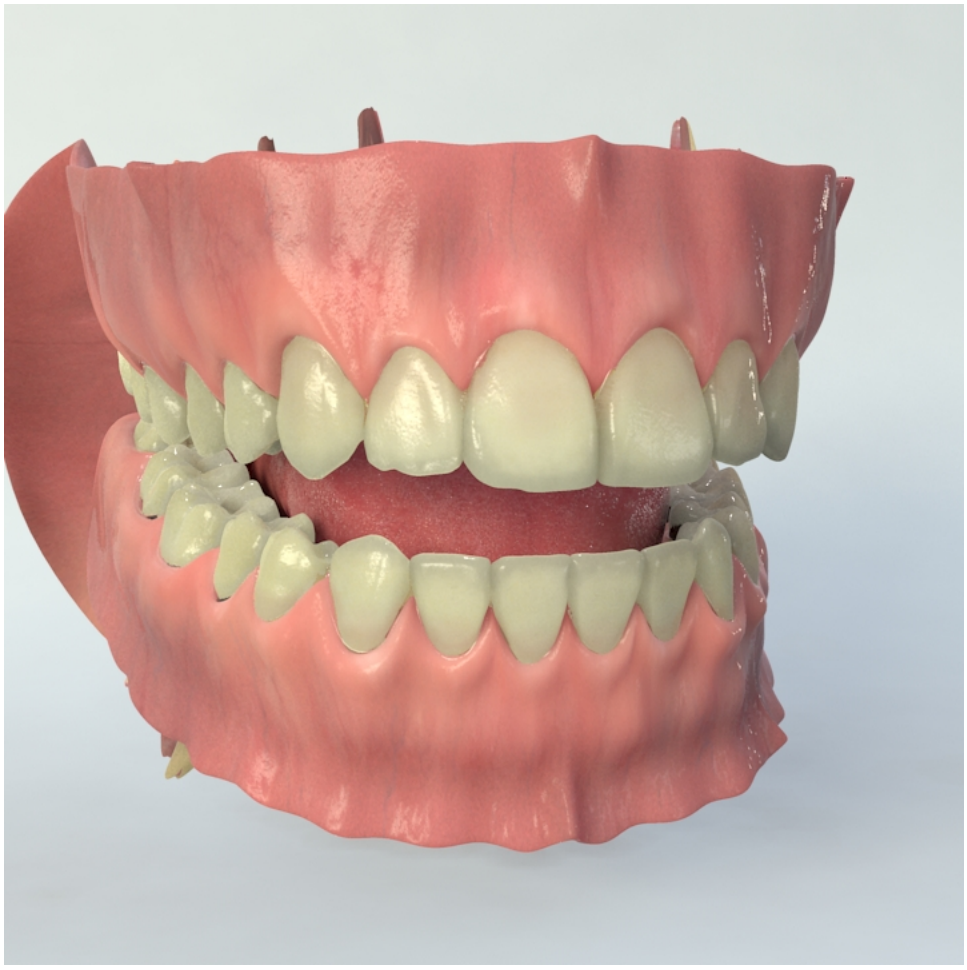

Figure 4.3: Non-physically processed teeth and mouth

To show the effects of back scattering, a camera was placed in the mouth. The upper teeth are back lit only and hence show only a pure scatter color. The lower teeth are lit from both sides, displaying a more blended appearance, as shown in Figure 4.4. Some pixelized and splotchy areas on the gums and the tongue are caused by the extremely close proximity of the camera here; the

textures applied cannot provide enough details to smoothly render the surface.


Figure 4.4: Back scatter of non-physically processed mouth

A dirt layer was added on top of the other layers (Figure 4.5) to simulate calculus. Since it was the first layer that eye rays reached, the dirt layer prevented the rays from deeply rendering the surface and, hence, affected light scattering. The amount of scattering is reduced, which also leads to a reduction of specular light. Additionally, the color of the light was changed to yellow after entering the surface. Further, if the calculus is thick enough to behave like a calcium compound, no specular light will be present in that area.

Figure 4.5: Non-physically processed mouth with thick tooth calculus

## 4.3 Character Results

The test character, Dobby from *Harry Potter*, was modeled by Julian Johnson and rigged by Joel Anderson. Simple textures for the head and eyes were created for visual appeal. Comparing Figure 4.6a with Figure 4.6b, shows a realistic light decay in the mouth, and realistic characteristics on both teeth and other mouth areas. Additionally, the model balances the lighting energy properly between diffuse, reflection and scattering.

(a) Indoor scene, cloudy (b) Outdoor Scene, sunny

Figure 4.6: Teeth rendered with character

# Chapter 5

# Conclusions and Future Work

## 5.1 Conclusions

Bert Paul, a CG supervisor at DreamWorks Animation, said recently that the biggest secret of processing mouths in the current movie industry is to keep them closed. CG teeth may appear realistic in alien or monster movies, but few do when rendering human characters because we see human teeth every day, and even small differences are easy to spot. The purpose of this thesis is to explore a possibly better process for rendering teeth and mouths in CG, based on current techniques.

This thesis has attempted to account for almost all factors regarding tooth shading and lighting in rendering CG characters. Among these factors, subsurface scattering was the most prominent. Several problems appeared during implementation, unexpectedly, such as the inherent imperfections of the misss_pysical shader. Also, due to lack of (animated) character models and scenes, the result could not be tested in more complex situations and animation; therefore, problems such as flickering and inconsistencies in dramatic lighting are difficult to predict. Other aspects, such as rendering time and pipeline issues have not been discussed due to lack of resources, although they are equally important when considering production work. Through the combination of art and technology, however, the research achieved a convincing result, and provided guidance for processing realistic human teeth in CG productions.

## 5.2 Possible Improvements

Due to time constraints and other factors, opportunities for improvements exist. Several possible and feasible ways to either increase efficiency or improve realism have emerged during the research.

### 5.2.1 Tools for Generating Inner Layer Models

As discussed in Chapter 3, actual layered models are critical if using physically correct methods, e.g., photon mapping, to shade teeth. Acquiring models of teeth from scanning currently remains unfeasible due to limitations in technology. Similarly, artistic models are inaccurate and extremely time-consuming to produce from observation, since models must incorporate multiple layers, and are therefore difficult to distinguish with intense light scattering. A reasonably accurate model including the outward shape of teeth, combined with empirical base data of layer distribution from the dental field, offers an acceptable compromise. From this data, scripting tools can aid in generating two inner model layers and the EDJ, and can possibly build the shading network for future rendering.

### 5.2.2 Customized 3D Textures and Light Rig

The main benefit of utilizing the class of non-physical shaders is to control the interaction between the scatter surface layers, or specifically to control the fall-off between dentin and pulp through scatter radii, scatter weights and scatter depth. If other components, such as diffuse, reflection and bump, can work correspondingly to the scatter layers, efficiency improvements and better rendering will result. Given this concept, a customized group of 3D textures, which are tunable with components that correlate to empirical base data, would be especially valuable in research and implementation. With the same visual goal, light-based solutions are also possible. In this approach, a light rig consisting of a number of volumetric lights illuminate the mouth and each tooth separately with customizable fall-off, achievable using a simple gobo. Additionally, this concept can ignore environmental lights, hence offering greater ability to control animation.

### 5.2.3 Significance of Environmental Impacts

Although much of the discussion focused on intrinsic properties of teeth, the final look is still largely affected by environmental factors in both physical and non-physical techniques. Factors that impact the mouth include skin color, saliva and light sources. Impacts on teeth include the colors of the gums and lips, surface humidity, calculus and light sources. For example, if using a physical approach, the photon color, energy and distribution must match the characteristics of the light source. Otherwise, a small amount of saliva on the surface of teeth could dramatically change the reflection compared with dry teeth. Heuristics combining these aspects would be helpful for production.

### 5.2.4 Customized Shader for Teeth

All future work discussed above is based to some extent on current technology and context, but also on a completely new approach, of developing a specialized shader for teeth, similar to those for skin. A few researchers have suggested in the past ten years to build models for shading and rendering teeth, either from a dental or a computer science perspective, but rarely achieved a believable result. This goal is certainly deserving of implementation, but will require resources from dentistry, physics and computer science for solving the awkwardness of perpetually closed mouths.

# Bibliography


[1] R. Diebolder R. Hibst A. Kienle F.K. Forster, "Light propagation in dentin: influence of microstructure on anisotropy", *Physics in Medicine and Biology* 2003.

[2] R. Hibst A. Kienle F. K. Forster, "Anisotropy of light propagation in biological tissue", *Optics Letters* 2004.

[3] R. Hibst A. Kienle R. Michels, "Magnification – a new look at a long-known optical property of dentin", *Journal of Dental Research* 2006.

[4] G.V.G. Baranoski A. Krishnaswamy, "A Biophysically-Based Spectral Model of Light Interaction with Human Skin", *Computer Graphics Forum* 2004.

[5] G.W. Alvin, "Description of color, color-replication process, and esthetics", *Contemporary fixed prosthodontics*, 2007.

[6] American Dental Association, "Dental Shade Guides", *The Journal of The American Dental Association* 2002.

[7] J.J. ten Bosch B. Angmar-Mansson, "Optical methods for the detection and quantification of caries", *Advances in Dental Research* 1989.

[8] N. Blevins, *CG Education*, 2006, URL: `http://www.neilblevins.com/cg_education/translucency/translucency.htm`.

[9] J.C. Coops J.J. ten Bosch, "Tooth Color and Reflectance as Related to Light Scattering and Enamel Hardness", *Journal of Dental Research* 1995.

[10] NVIDIA Corporation, *mental ray 2013 documentation*, 2013, URL: `http://docs.autodesk.com/MENTALRAY/2013/ENU/mental-ray-help/,2013`.

[11] J.J. ten Bosch D. Spitzer, "The absorption and scattering of light in bovine and human dental enamel", *Calcif Tissue Res* 1975.

[12] O. Tric M.J. Anderson M. Tourville A. Kobashigawa D.A. Terry W. Geller, "Anatomical form defines color: function, form, and aesthetics", *Pract Proced Aesthet Dent* 2002.

[13] Alternative Dentist, *Structure of Gums*, 2006, URL: `http://www.excellentpatientcare.com/home-care-dentist-charlotte-nc.html`.

[14] J.D.B. Featherstone W. Seka F. Daniel E.G. Richard, "Nature of light scattering in dental enamel and dentin at visible and near-infrared wavelengths", *Applied Optics* 1995.

[15] G.E. King G.B. Jr. Pelleu G.J. Barna J.W. Taylor, "The influence of selected light intensities on color perception within the color range of natural teeth", *J Prosthet Dent.* 1981.

[16] L. Marc H. Pat H.W. Jensen R.M. Stephen, "A Practical Model for Subsurface Light Transport", *ACM SIGGRAPH 2001*, Los Angeles, CA, 2001.

[17] J. Rudolf J.R. Zijp, "Optical properties of dental hard tissues", PhD dissertation, Faculty of Mathematics and Natural Sciences, 2001.

[18] R.A.J. Groenhuis J.R. Zijp J.J. ten Bosch, "HeNe-Laser Light Scattering by Human Dental Enamel", *Journal of Dental Research* 1995.

[19] Pawlina M.H. Ross G.I. Kaye, *Histology: A Text and Atlas. With Correlated Cell and Molecular Biology*, 2006.

[20] P.L. Fan J.G. Frazer-DIB R. Yu R.H.W. Brodbelt W.J. O'Brien, "Translucency of Human Dental Enamel", *Journal of Dental Research* 1981.

[21] M. Bailey S. Shetty, "A Physical Rendering Model for Human Teeth", *ACM SIGGRAPH 2010*, Los Angeles, CA, 2010.

[22] S.A. Prahl S.L. Jacques, *Introduction to Biomedical Optics*, 2002, URL: `http://omlc.ogi.edu/classroom/ece532/`.

[23] H.C. Kucukesmen P. Sema Aka S.S. Atsu M.A. Kilicarslan, "Effect of zirconium-oxide ceramic surface treatments on the bond strength to adhesive resin", *The Journal of Prosthetic Dentistry* 2006.

[24] C. Thomas S.T. Abedon P. Hyman, "Human Teeth With and Without Caries Studied by Laser Scattering, Fluorescence, and Absorption Spectroscopy", *IEEE Journal of Quantum Electronics* 1984.

[25] V.N. Grisimov V.M. Zolotarev, "Architectonics and Optical Properties of Dentin and Dental Enamel", *Optics and Spectroscopy* 2001.

[26] Wikipedia, *Dentin*, 2012, URL: `http://en.wikipedia.org/wiki/Dentin`.

[27] Wikipedia, *Labeledandfulltooth*, 2012, URL: `http://en.wikipedia.org/wiki/File:Labeledandfulltooth.jpg`.

[28] Wikipedia, *Refractive Index*, 2012, URL: `http://en.wikipedia.org/wiki/Refractive_index`.

[29] Wikipedia, *Color Management*, 2013, URL: `http://en.wikipedia.org/wiki/Color_management`.

[30] Wikipedia, *SRGB*, 2013, URL: `http://en.wikipedia.org/wiki/Srgb`.

[31] J.F. de Boer Y. Zhang D.H. Pashley J.S. Nelson X.J. Wang T.E. Milner, "Characterization of dentin and enamel by use of optical coherence tomography", *Applied Optics* 1999.